THE JOURNAL OF PHYSICAL CHEMISTRY Letters

Letter

pubs.acs.org/JPCL

Ultrafast Charge-Transfer Dynamics in the Iron–Sulfur Complex of *Rhodobacter capsulatus* Ferredoxin VI

Ziliang Mao, Elizabeth C. Carroll,[‡] Peter W. Kim,[§] Stephen P. Cramer,[*] and Delmar S. Larsen[*]

Department of Chemistry, University of California Davis, One Shields Avenue, Davis, California 95616, United States

Supporting Information

ABSTRACT: Iron–sulfur proteins play essential roles in various biological processes. Their electronic structure and vibrational dynamics are key to their rich chemistry but nontrivial to unravel. Here, the first ultrafast transient absorption and impulsive coherent vibrational spectroscopic (ICVS) studies on 2Fe–2S clusters in *Rhodobacter capsulatus* ferredoxin VI are characterized. Photoexcitation initiated populations on multiple excited electronic states that evolve into each other in a long-lived charge-transfer state. This suggests a potential light-induced electron-transfer pathway as well as the possibility of using iron–sulfur proteins as photosensitizers for light-dependent enzymes. A tyrosine chain near the active site suggests potential hole-transfer pathways and affirms this electron-transfer pathway. The ICVS data revealed vibrational bands at 417 and 484 cm^{-1}, with the latter attributed to an excited-state mode. The temperature dependence of the ICVS modes suggests that the temperature effect on protein structure or conformational heterogeneities needs to be considered during cryogenic temperature studies.

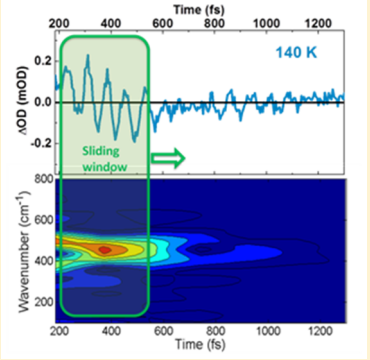

Iron–sulfur (FeS) clusters are ubiquitous in nature and serve a wide range of functions, including electron transfer (ET), small-molecule sensing, and the catalysis of chemical reactions.[1] They also play key roles in various essential biological processes such as photosynthesis, cellular respiration, and nitrogen fixation.[2] Since their discovery in the 1960s, FeS cluster proteins have been studied extensively, yet key questions about their structure–function paradigm remain. While it is clear that their electronic structure is essential for their rich chemistry, it is nontrivial to characterize due to its complexity and the fact that a large number of states exist in close proximity.[3,4]

Recently, interest in photoinduced chemical processes involving FeS proteins has risen. For example, the involvement of FeS clusters in photosensitization in living cells[5] and photoinduced ET in the purple phototroph *Rhodoferax fermentans*[6] has been reported. The incorporation of external photosensitizers to hydrogenases and nitrogenases enabled photoactivated hydrogen production and nitrogen fixation.[7−9] Similarly, several Fe–Fe hydrogenase model compounds that contain FeS clusters were found to facilitate hydrogen production under sunlight without adding external photosensitizers.[10] This opens the possibility of using FeS proteins and model compounds as photosensitizers for solar hydrogen production.

Of the many varied FeS clusters identified in nature, the 2Fe–2S clusters are the simplest multi-iron clusters for study. A representative protein that binds a 2Fe–2S cluster is the sixth ferredoxin (Rc6) discovered from *Rhodobacter capsulatus*,[11] which is involved in the synthesis of FeS clusters.[12] Its structure has been determined (Figure 1)[12] and resembles structures typical of 2Fe–2S ferredoxins that are critical ET proteins involved in a range of metabolic processes. Hence, Rc6 is an excellent model system for the time-resolved characterization of photoinduced dynamics in FeS clusters.

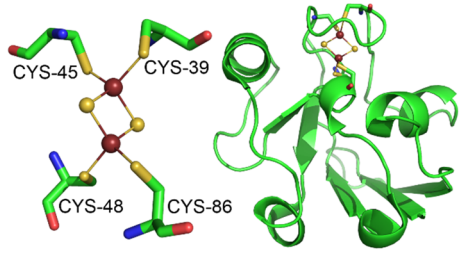

Figure 1. Oxidized Rc6 active site structure. (Left) 2Fe–2S cluster structure and (Right) full protein structure (PDB: 1E9M). Colors for atoms: Fe (brick), S (yellow), C (green), N (blue), and O (red).

Here, we report the first ultrafast transient absorption (TA) study on the electronic relaxation dynamics and impulsive coherent vibrational spectroscopic (ICVS) study on the vibrational relaxation dynamics of oxidized Rc6. We have used these techniques to obtain better knowledge of the electronic and vibrational dynamics of the 2Fe–2S cluster. The TA technique probes the time-dependent change of sample absorbance upon laser excitation and reveals information about excited-state population evolution, electron and proton transfer, and subsequent dynamics. The ICVS technique is a variant TA technique and has been used to study the vibrational dynamics of the mononuclear Fe site (1Fe–4S) in the *Pyrococcus furiosus* rubredoxin (*Pf*Rd) and the 7Fe–9S–1Mo cofactor (FeMoco)

Received: August 2, 2017
Accepted: September 5, 2017
Published: September 5, 2017

DOI: 10.1021/acs.jpclett.7b02026
J. Phys. Chem. Lett. 2017, 8, 4498–4503

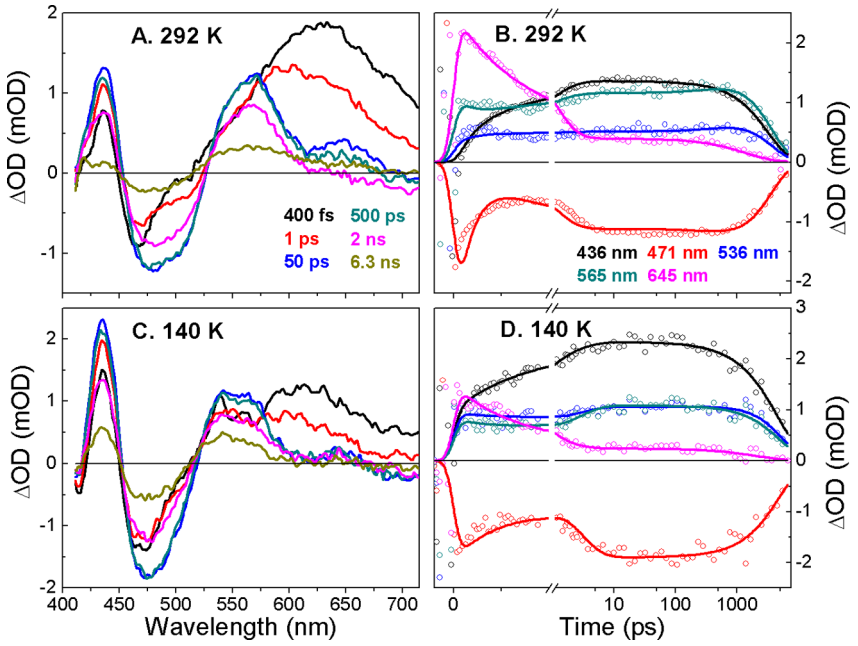

Figure 2. Transient spectra at select probe times [(A) for 292 K and (C) for 140 K] and kinetics at select wavelengths [(B) for 292 K and (D) for 140 K]. For panels (B) and (D), the open circles are for the raw data and the solid curves are fits to the raw data using the sequential model in Figure 3.

of the nitrogenase MoFe protein from *Azotobacter vinelandii*.[13−15] These studies identified key vibrational modes that are coupled to excited electronic states that participate in photoinduced ET processes.

To refine the models for the electronic and vibrational dynamics, cryogenic temperature (140 K) study was also performed to complement room-temperature study. Lower temperature slows down the relaxation of excited-state dynamics as well as the dephasing of vibrational wave packets and allows more refined characterization of the kinetics. Because most static spectroscopic studies on FeS proteins have been conducted at cryogenic temperatures, the 140 K study also establishes a point of comparison to previous studies.

The TA spectra of Rc6 at select delay times at both 292 and 140 K are contrasted in Figure 2A,C with corresponding kinetics at select wavelengths in Figure 2B,D. The kinetics are distinctly nonmonotonic, with dynamics extending over multiple time scales from fs to ns. The results are thus more complicated than the TA dynamics observed in the 1Fe−4S *Pf*Rd and FeMoco in nitrogenase MoFe protein.[13,15] At both temperatures, multiple contributions to the TA signals are observed: (1) a ground-state bleaching band at 460 nm; (2) a negative band at 480 nm; (3) a positive signal at around 436 nm that appears immediately after excitation and persists for several ns; (4) a positive band at around 565 nm at 292 K and 545 nm at 140 K; it appears earlier or stronger at 140 K, where it grows in several ps and then decays away after 6 ns; and (5) a broad positive signal at around 645 nm that is blue-shifted at 140 K relative to 292 K; it grows in within 100 fs and decays away after 1 ns.

Analysis of broad-band TA signals was performed using a multicomponent global analysis method.[16,17] A simple four-compartment sequential model was adopted to fit the data to estimate the underlying directly observed time scales in the data (Figure 3). This model fits the TA signals well (Figure 2), suggesting that (at least) four populations are resolved in the data. Although the evolution associated difference spectra

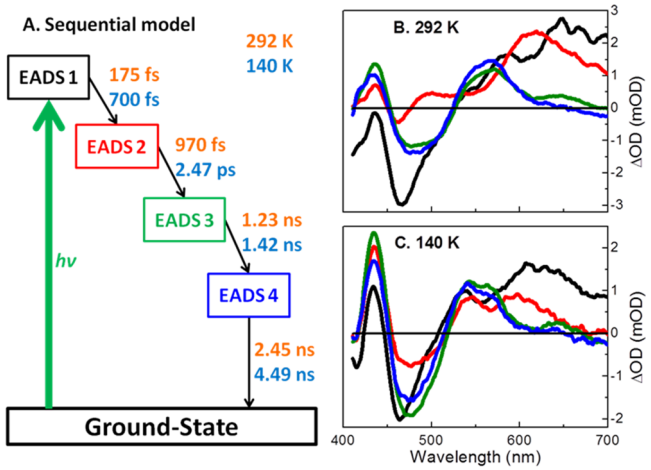

Figure 3. (A) Four-compartment sequential model to describe the data. Time constants for 292 K are in orange, and those at 140 K are in cyan. (B,C) Extracted EADS for the fit of the sequential model to the 292 K (B) and 140 K (C) data. The evolution profiles for these EADS are contrasted in Figure S4. The colors of the EADS are the same as those in panel (A): EADS1 (black), EADS2 (red), EADS3 (olive), and EADS4 (blue).

(EADS) extracted from this analysis are not the actual spectra of the constituent populations, this anlysis serves as a useful measure to interpret the time scale and nature of the underlying dynamics (Figure 3B,C). Unfortunately, efforts to construct more "correct" models were unsuccessful and can be reviewed in the Supporting Information (Figures S6 and S7).

As expected, the dynamics at 140 K are slower than the 292 K dynamics (Table S1).[18] The EADS of the sequential model (Figure 3B,C) share similar spectral characteristics with the raw TA spectra (Figure 2A,C). They all exhibit ground-state bleach and stimulated emission features at 460 and 480 nm, with excited-state absorption bands near 436 nm and in the long-

DOI: 10.1021/acs.jpclett.7b02026
J. Phys. Chem. Lett. 2017, 8, 4498−4503

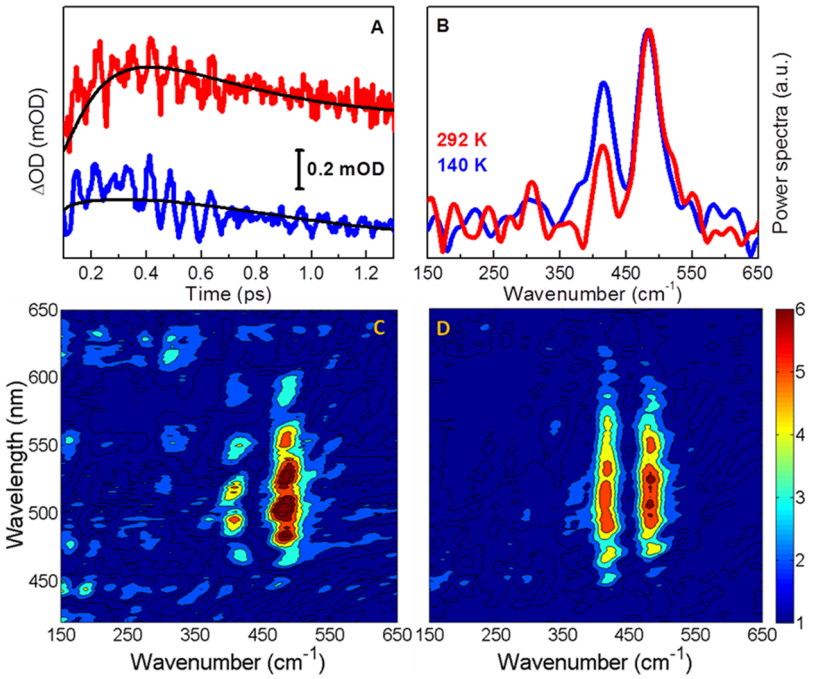

Figure 4. (A) Oscillatory components and fits using the target model proposed in Figure S6 for the 525 nm probe wavelength at 292 K (red) and 140 K (blue). (B) Power spectra obtained for the 525 nm probe wavelength at 292 K (red) and 140 K (blue). (C) 2D power spectra at 292 K. (D) 2D power spectra at 140 K. Only the kinetics within the first 2 ps following laser excitation were collected for investigation of the vibrational relaxation dynamics of Rc6.

wavelength region. The EADS3 and EADS4 are nearly identical below 600 nm, with two positive bands at 436 and 565 nm. These bands decay on the same time scale (Figure S5) and may represent either the same species or two species that are in equilibrium. We also notice that the 436 nm band is formed instantly and continues to grow within the first 2 ps, while a long-wavelength band near 625 nm forms instantly and decays away within 5 ps. This is suggestive that there may be multiple excited-state populations that initially coexist from the excitation pulse and then evolve from one into the other. The 471 and 565 nm kinetics both exhibit nonmonotonic kinetics. The initial decay has a time constant of 175 fs at 292 K that slows to 700 fs at 140 K (well outside of our 125 fs instrumental response). At the far-red region near 645 nm, we can see from both the kinetics and the EADS3 and EADS4 that the 645 nm band decays while the 565 nm grows on the 2−4 ns time scale.

These data and the EADS analysis are supportive of an inhomogeneous set of populations involved in the photodynamics with evolution from one state to another. On the basis of the EADS analysis and given the fact that there are multiple closely spaced charge-transfer transitions in the pump wavelength region of the steady-state absorption spectra of 2Fe−2S ferredoxins,[3,4] efforts were made to analyze and interpret the TA data using a more complex four-state combined inhomogeneous parallel-sequential target model (Figures S6 and S7). In this model, the pump laser excites the 2Fe−2S cluster to three different excited states simultaneously, with the higher states decaying to their nearest lower states. Details of this model can be found in the Supporting Information.

For the ICVS experiment, the 2Fe−2S cluster in Rc6 was excited at 525 nm. The time-dependent absorption changes were observed over a broad wavelength region from 400 to 700 nm. The pump pulse excites the S → Fe ligand-to-metal charge-transfer transitions in the 2Fe−2S cluster[3] of Rc6 and promotes a faction of the molecules to electronic excited states, where coherent vibrational wave packets are launched.[19] The kinetics of the ICVS data are nearly identical to the TA signals in Figure 2 but overlaid with oscillatory components decaying within a few picoseconds. Unfortunately, the cross-phase modulation artifact[20] lasts for about 100 fs (Figure S3) and prevents the characterization of <100 fs dynamics, and we limited our analysis to time delays longer than 100 fs.

Figure 4A contrasts the ICVS kinetic traces for the 525 nm probe wavelength at both 292 and 140 K with baseline fits. To separate the oscillatory components of these signals from the population dynamics discussed above, the target model proposed in Figure S6 for the TA study was used to fit the ICVS data (black curves in Figure 4A), and the fitting curves are subtracted from the raw data to obtain the residuals (Figure S8). Fourier transform (FT) analysis was performed on the residuals, and the resulting maps of the FT power spectra of the residuals at both 292 and 140 K are shown in Figure 4C,D. From the 2D maps, two positive bands at 484 and 417 cm^{-1} for both 292 and 140 K are clearly resolved. However, the intensity of the 484 cm^{-1} band increased significantly at 140 K compared to that at 292 K. At some probe wavelength, the 417 cm^{-1} peak almost disappeared at 292 K. The FT intensity spectra for the 525 nm probe wavelength are shown in Figure 4B, which shows the same temperature effect as the 2D maps.

The 417 cm^{-1} band in the 140 K ICVS data is consistent with resonance Raman and normal mode calculations for Rc6 at 77 K,[21] as well as for other 2Fe−2S ferredoxins such as putidaredoxin[22] and *Aquifex aeolicus* ferredoxin 5.[21] It was assigned as the $B_{2u}{}^{b}$ asymmetric Fe−S^{b} stretching mode in idealized D_{2h} symmetry for the $Fe_2S^{b}{}_2S^{t}{}_4$ core.[21,22]

DOI: 10.1021/acs.jpclett.7b02026
J. Phys. Chem. Lett. 2017, 8, 4498−4503

The 484 cm^{-1} band has not been reported in the 2Fe−2S ferredoxin resonance Raman spectra nor in more recent IR difference spectra.[23] It is a higher frequency than most of the Fe−S related normal modes, but it also does not align as a combination band.[24] Instead, a similar band near this frequency has been observed in room-temperature ICVS studies of *Pf*Rd[13] and blue Cu proteins.[25,26] In both samples, it was attributed to excited-state vibrations.

To investigate the nature of these modes, a sliding window Fourier transform (SWFT)[13] of the oscillatory components of the signal was performed on the ICVS data (Figure 5). The 484

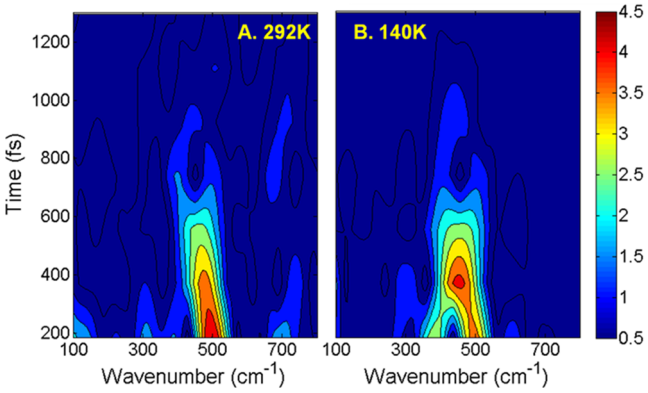

Figure 5. Spectrogram obtained by performing the SWFT of the oscillatory component of the signal at a 525 nm probe wavelength at (A) 292 and (B) 140 K. The calculations used a sixth-order super Gaussian function and 370 fs window.

cm^{-1} band is initially observed at higher frequency but slowly shifts to lower frequency within ~600 ps at both temperatures. This is consistent with the multiple excited-state populations that evolve from one state into another. It is likely that the wave packet evolves from the highest excited electronic state potential energy surface to the lower-lying states after excitation. Because the electronic structure of the active site differs at different electronic states, it is reasonable to observe shifting of the vibrational frequency of the excited-state vibrations. Similar phenomena have been reported before.[27] The SWFT also shows that the 417 cm^{-1} band has a slightly longer lifetime and appears slightly later than the 484 cm^{-1} band, suggesting an assignment of the 484 cm^{-1} band to a rapidly decaying excited state. However, the difference in lifetimes was not significant enough for a decisive conclusion.

The temperature dependence of the relative intensity or existence of the two vibrational bands was surprising to observe. Fraser and co-workers recently reported that cryocooling suppresses or modifies protein conformation heterogeneities.[28] We postulate that the temperature change either slightly perturbs the structure/geometry of the active site and its surrounding amino acids of Rc6 or that different temperature favors different conformations of the protein and thus affects the relative intensity or existence of the vibrational modes observed. This phenomenon suggests that the temperature effect on the structure or conformation heterogeneities of FeS proteins needs to be carefully considered when interpreting experimental data often collected at cryogenic temperatures (e.g., EPR, cryo-FTIR, and Mossbauer spectroscopies).

The TA signals argue that laser excitation of the 2Fe−2S cluster of Rc6 generates multiple excited-state populations, which result in complicated multiphasic dynamics. This is not surprising because there are multiple charge-transfer transitions proposed from electronic structure calculations in the visible region for 2Fe−2S clusters[3,4] and the bandwidth of the pump laser overlaps with several of them (Figure 6A). As early as

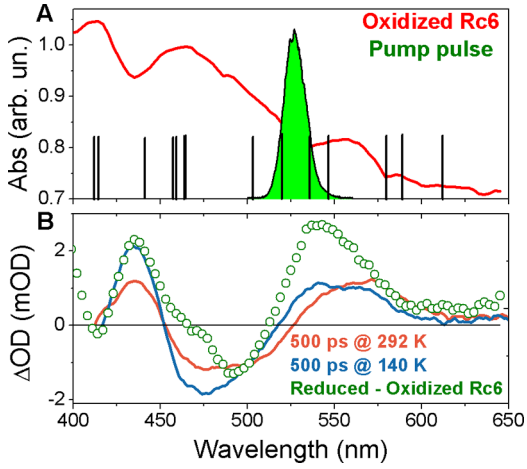

Figure 6. (A) Static absorption spectrum for oxidized Rc6 (red) overlaid with the pump laser spectrum (green). The vertical black bars are the charge-transfer bands predicted by Noodleman et al.,[3] and the blue curved arrows indicate excited-state population transfers following laser excitation. (B) TA spectra at 500 ps for 292 K (orange) and 140 K (cyan) overlaid with the static difference absorption spectrum (olive, open circles) obtained by subtracting the absorption spectrum of oxidized Rc6 from that of reduced Rc6. Static absorption spectra data were taken from Sainz et al., 2006.[12]

1984, Noodleman and co-workers calculated dozens of electronic transitions for the near-IR and visible region alone.[3] According to Noodleman's predictions, the three charge-transfer bands that were excited by the 525 nm pump (Figure 6A) are 519 nm (opp. S, S* → Fe), 536 nm (opp. S, S* → Fe), and 546 nm (S, S*→ Fe).[3] More recently, Neese and co-workers suggested that the simple double-exchange model underestimates the true density of low-lying states by 1−2 orders of magnitude, which further complicates the interpretation of photoinduced dynamics in these systems.[4]

The simultaneous excitation of several excited-state populations also indicates that during the ICVS experiment multiple wave packets are simultaneously launched on multiple electronic states. This might be a disadvantage if the vibrations on a single excited electronic state of FeS proteins are to be studied. However, it allows us to observe vibrational modes on multiple electronic excited states and provides helpful information for theoretical simulations of excited-state vibrations in FeS clusters. In particular, these modes are not accessible by steady-state vibrational techniques such as resonance Raman that are primarily sensitive to ground-state vibrations.

The long lifetimes of the lower excited electronic states (2.45 ns for 292 K and 4.49 ns for 140 K) are significantly longer than those of *Pf*Rd[13] and FeMoco[14] in the nitrogenase MoFe protein, suggesting that 2Fe−2S clusters like those in Rc6 are potential candidates as external photosensitizers for light-induced hydrogen production in hydrogenase or hydrogenase model compounds.[9] The longer the lifetimes of these charge-transfer populations, the greater the opportunity to take advantage of them for productive redox chemistry like light-induced hydrogen generation. The proximity of the 2Fe−2S

DOI: 10.1021/acs.jpclett.7b02026
J. Phys. Chem. Lett. 2017, 8, 4498−4503

cluster to the protein surface (Figure S9) also makes it easier to use 2Fe−2S clusters as photosensitizers.

The TA data together with the EADS and extracted time scales (Table S1) and target analyses suggest that there are clearly two long-lived states that coexist (Figures 2 and 3). One resembles the 500 ps TA spectrum shown in Figure 6B, whereas the other is a positive band at 645 nm. The 645 nm band decays within 1.5 ns, but the other population persists up to 2.45 ns at 292 K and 4.49 ns at 140 K. Interestingly, the TA spectra at 500 ps for both temperatures strongly resemble the reduced−oxidized steady-state difference spectra (Figure 6B). This suggests that the longer-lived state is probably due to a photoinduced long-range "external" ET transition illustrated by Scheme 1 (ET Path 2). This is in agreement with the electronic

Scheme 1. Proposed ET and HT Pathways[a]

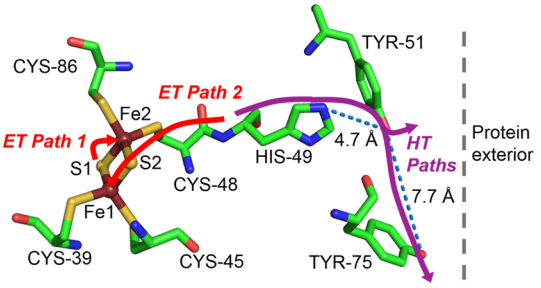

[a]Color coding: ET pathways are denoted with red arrows, and HT pathways with purple arrows.

structure calculations by Noodleman et al.,[3] where the 525 nm pump laser excites the ET transitions from the opposite cysteine-thiol to an iron (Opp. S → Fe). It is possible that the pump laser induces a transient reduction of the 2Fe−2S cluster by promoting one electron to move from a cysteine-thiol to the opposite iron while another electron from a nearby amino acid fills the hole on the cysteine. After laser excitation, the electron returns to its original location. This partial reduction persists for a few ns and is consistent with the larger barrier for a long-range ET from an external amino acid to the cysteine-thiol and then to an opposite iron. To further investigate this long-range "external" ET pathway, efforts were made to identify potential hole-transfer (HT) pathways in Rc6 because ET from amino acids requires the quenching of holes. Recently, HT pathways in proteins have been investigated in multiple metalloproteins where linear/branched chains of tryptophan and tyrosine residues serve as potential HT pathways due to their lower redox potentials through changing their protonized states.[29−31] Close examination of the crystal structure of Rc6 reveals that Cys48 is directly bonded with His49, whose imidazole side chain is only 4.7 Å from the aromatic ring of Tyr51. The latter is 7.7 Å from Tyr75, and both Tyr51 and Tyr75 are close to the protein surface (Scheme 1). Thus, the electron holes created by the long-range ET can be quenched through the HT pathways: Cys48 → His49 → Tyr51 (and/or → Tyr75) (Scheme 1). The Trp56 residue of Rc6 is more than 16 Å from the active site and surrounding amino acids and thus does not participate in the HT pathways. The shorter-lived state (1.23 ns for 292 K and 1.42 ns for 140 K) may be attributed to the transient internal ET from a bridging sulfide or a neighboring cysteine-thiol to iron (ET Path 1 in Scheme 1). These results suggest that a potential light-induced long-range ET pathway might exist in 2Fe−2S ferredoxins. Similar photoinduced ET pathways have been observed in other ET metalloenzymes.[6,26,32]

To conclude, the ultrafast electronic and vibrational relaxation dynamics of Rc6 were characterized. The TA signals revealed that multiple ligand-to-metal charge-transfer populations were induced by laser excitation that evolve into low-lying states. Two long-lived states were identified, with the longer one attributed to a long-range *external* ET, which suggests the potential existence of a photoinduced long-range ET pathway in FeS proteins. The existence of potential HT pathways consisting of a chain of histidine and tyrosines near Cys48 affirms the existence of this long-range ET pathway. The shorter-lived state is ascribed to a transient *internal* ET from a nearby sulfur to iron. The excited-state population transfer is consistent with the slight shifting of the 484 cm^{-1} ICVS band first observed in Rc6 and attributed to excited electronic state vibrations. Exactly how this band may contribute to ET and redox properties of FeS clusters is a topic of further study (manuscript in preparation). The temperature effect to the ICVS spectra suggests that the temperature effect deserves consideration during the study of FeS proteins at cryogenic temperatures. The study of 2Fe−2S ferredoxins' ultrafast electronic and vibrational dynamics lays a foundation for future characterization of larger FeS clusters in proteins.

■ ASSOCIATED CONTENT

Supporting Information

The Supporting Information is available free of charge on the ACS Publications website at DOI: 10.1021/acs.jpclett.7b02026.

Experimental procedures, experimental setup diagrams, details about global analysis, and supporting results (PDF)

■ AUTHOR INFORMATION

Corresponding Authors

*E-mail: dlarsen@ucdavsi.edu (D.S.L.).
*E-mail: spjcramer@ucdavis.edu (S.P.C.).

ORCID

Delmar S. Larsen: 0000-0003-4522-2689

Present Addresses

‡E.C.C.: Department of Imaging Physics, Delft University of Technology, Postbus 5, 2600 AA Delft, The Netherlands.
§P.W.K.: Applied Biosciences and Engineering, Sandia National Laboratories, Livermore, CA 94550, U.S.A.

Notes

The authors declare no competing financial interest.

■ ACKNOWLEDGMENTS

We thank Jacques Meyer from CEA-Grenoble in France for generously providing the Rc6 sample. This work was funded by NSF CHE-1413739 (D.S.L.), NSF CHE-0745353 (S.P.C.), NSF CHE-1308384 (S.P.C.), and NIH GM65440 (S.P.C.).

■ REFERENCES

(1) Lill, R. Function and biogenesis of iron-sulphur proteins. *Nature* **2009**, *460* (7257), 831−838.
(2) Johnson, D. C.; Dean, D. R.; Smith, A. D.; Johnson, M. K. Structure, function, and formation of biological iron-sulfur clusters. *Annu. Rev. Biochem.* **2005**, *74*, 247−281.
(3) Noodleman, L.; Baerends, E. J. Electronic-Structure, Magnetic-Properties, Electron-Spin-Resonance, and Optical-Spectra for 2-Fe

DOI: 10.1021/acs.jpclett.7b02026
J. Phys. Chem. Lett. 2017, 8, 4498−4503

Ferredoxin Models by Lcao-X-Alpha Valence Bond Theory. *J. Am. Chem. Soc.* **1984**, *106* (8), 2316−2327.
(4) Sharma, S.; Sivalingam, K.; Neese, F.; Chan, G. K. L. Low-energy spectrum of iron-sulfur clusters directly from many-particle quantum mechanics. *Nat. Chem.* **2014**, *6* (10), 927−933.
(5) Kim, C. S.; Jung, J. Iron Sulfur Centers as Endogenous Blue-Light Sensitizers in Cells - a Study with an Artificial Nonheme Iron Protein. *Photochem. Photobiol.* **1992**, *56* (1), 63−68.
(6) Hochkoeppler, A.; Zannoni, D.; Ciurli, S.; Meyer, T. E.; Cusanovich, M. A.; Tollin, G. Kinetics of photo-induced electron transfer from high-potential iron-sulfur protein to the photosynthetic reaction center of the purple phototroph Rhodoferax fermentans. *Proc. Natl. Acad. Sci. U. S. A.* **1996**, *93* (14), 6998−7002.
(7) Brown, K. A.; Dayal, S.; Ai, X.; Rumbles, G.; King, P. W. Controlled Assembly of Hydrogenase-CdTe Nanocrystal Hybrids for Solar Hydrogen Production. *J. Am. Chem. Soc.* **2010**, *132* (28), 9672−9680.
(8) Brown, K. A.; Harris, D. F.; Wilker, M. B.; Rasmussen, A.; Khadka, N.; Hamby, H.; Keable, S.; Dukovic, G.; Peters, J. W.; Seefeldt, L. C.; King, P. W. Light-driven dinitrogen reduction catalyzed by a CdS:nitrogenase MoFe protein biohybrid. *Science* **2016**, *352* (6284), 448−450.
(9) Adam, D.; Bosche, L.; Castaneda-Losada, L.; Winkler, M.; Apfel, P.; Happe, T. Sunlight-Dependent Hydrogen Production by Photosensitizer/Hydrogenase Systems. *ChemSusChem* **2017**, *10* (5), 894−902.
(10) Wang, W. G.; Rauchfuss, T. B.; Bertini, L.; Zampella, G. Unsensitized Photochemical Hydrogen Production Catalyzed by Diiron Hydrides. *J. Am. Chem. Soc.* **2012**, *134* (10), 4525−4528.
(11) Armengaud, J.; Meyer, C.; Jouanneau, Y. A [2Fe−2S] ferredoxin (FdVI) is essential for growth of the photosynthetic bacterium Rhodobacter capsulatus. *J. Bacteriol.* **1997**, *179* (10), 3304−3309.
(12) Sainz, G.; Jakoncic, J.; Sieker, L. C.; Stojanoff, V.; Sanishvili, N.; Asso, M.; Bertrand, P.; Armengaud, J.; Jouanneau, Y. Structure of a [2Fe−2S] ferredoxin from Rhodobacter capsulatus likely involved in Fe-S cluster biogenesis and conformational changes observed upon reduction. *JBIC, J. Biol. Inorg. Chem.* **2006**, *11* (2), 235−246.
(13) Tan, M. L.; Bizzarri, A. R.; Xiao, Y. M.; Cannistraro, S.; Ichiye, T.; Manzoni, C.; Cerullo, G.; Adams, M. W. W.; Jenney, F. E.; Cramer, S. P. Observation of terahertz vibrations in Pyrococcus furiosus rubredoxin via impulsive coherent vibrational spectroscopy and nuclear resonance vibrational spectroscopy - interpretation by molecular mechanics. *J. Inorg. Biochem.* **2007**, *101* (3), 375−384.
(14) Delfino, I.; Cerullo, G.; Cannistraro, S.; Manzoni, C.; Polli, D.; Dapper, C.; Newton, W. E.; Guo, Y. S.; Cramer, S. P. Observation of Terahertz Vibrations in the Nitrogenase FeMo Cofactor by Femtosecond Pump-Probe Spectroscopy. *Angew. Chem., Int. Ed.* **2010**, *49* (23), 3912−3915.
(15) Maiuri, M.; Delfino, I.; Cerullo, G.; Manzoni, C.; Pelmenschikov, V.; Guo, Y. S.; Wang, H. X.; Gee, L. B.; Dapper, C. H.; Newton, W. E.; Cramer, S. P. Low frequency dynamics of the nitrogenase MoFe protein via femtosecond pump probe spectroscopy - Observation of a candidate promoting vibration. *J. Inorg. Biochem.* **2015**, *153*, 128−135.
(16) van Stokkum, I. H. M.; Larsen, D. S.; van Grondelle, R. Global and target analysis of time-resolved spectra. *Biochim. Biophys. Acta, Bioenerg.* **2004**, *1657* (2−3), 82−104.
(17) Holzwarth, A. R. Data Analysis of Time-Resolved Measurements. In *Biophysical Techniques in Photosynthesis*; Amesz, J., Hoff, A. J., Eds.; Springer: Dordrecht, The Netherlands, 1996; pp 75−92.
(18) Larson, E. J.; Johnson, C. K. Temperature-dependent study of the ultrafast photophysics of all-trans retinal. *J. Phys. Chem. B* **1999**, *103* (49), 10917−10923.
(19) Fragnito, H. L.; Bigot, J. Y.; Becker, P. C.; Shank, C. V. Evolution of the Vibronic Absorption-Spectrum in a Molecule Following Impulsive Excitation with a 6 Fs Optical Pulse. *Chem. Phys. Lett.* **1989**, *160* (2), 101−104.
(20) Kovalenko, S. A.; Dobryakov, A. L.; Ruthmann, J.; Ernsting, N. P. Femtosecond spectroscopy of condensed phases with chirped supercontinuum probing. *Phys. Rev. A: At., Mol., Opt. Phys.* **1999**, *59* (3), 2369−2384.
(21) Xiao, Y. M.; Tan, M. L.; Ichiye, T.; Wang, H. X.; Guo, Y. S.; Smith, M. C.; Meyer, J.; Sturhahn, W.; Alp, E. E.; Zhao, J. Y.; Yoda, Y.; Cramer, S. P. Dynamics of Rhodobacter capsulatus [2Fe−2S] ferredoxin VI and Aquifex aeolicus ferredoxin 5 via nuclear resonance vibrational spectroscopy (NRVS) and resonance Raman spectroscopy. *Biochemistry* **2008**, *47* (25), 6612−6627.
(22) Fu, W. G.; Drozdzewski, P. M.; Davies, M. D.; Sligar, S. G.; Johnson, M. K. Resonance Raman and Magnetic Circular-Dichroism Studies of Reduced [2Fe−2S] Proteins. *J. Biol. Chem.* **1992**, *267* (22), 15502−15510.
(23) Khalil, M.; Bernhardt, R.; Hellwig, P. Raman and infrared spectroscopic evidence for the structural changes of the 2Fe−2S cluster and its environment during the interaction of adrenodoxin and adrenodoxin reductase. *Spectrochim. Acta, Part A* **2017**, *183*, 298−305.
(24) Han, S.; Czernuszewicz, R. S.; Kimura, T.; Adams, M. W. W.; Spiro, T. G. Fe2s2 Protein Resonance Raman-Spectra Revisited - Structural Variations among Adrenodoxin, Ferredoxin, and Red Paramagnetic Protein. *J. Am. Chem. Soc.* **1989**, *111* (10), 3505−3511.
(25) Cimei, T.; Bizzarri, A. R.; Cerullo, G.; De Silvestri, S.; Cannistraro, S. Excited state charge-transfer dynamics study of poplar plastocyanin by ultrafast pump-probe spectroscopy and molecular dynamics simulation. *Biophys. Chem.* **2003**, *106* (3), 221−231.
(26) Book, L. D.; Arnett, D. C.; Hu, H. B.; Scherer, N. F. Ultrafast pump-probe studies of excited-state charge-transfer dynamics in blue copper proteins. *J. Phys. Chem. A* **1998**, *102* (23), 4350−4359.
(27) Kobayashi, T.; Saito, T.; Ohtani, H. Real-time spectroscopy of transition states in bacteriorhodopsin during retinal isomerization. *Nature* **2001**, *414* (6863), 531−534.
(28) Keedy, D. A.; van den Bedem, H.; Sivak, D. A.; Petsko, G. A.; Ringe, D.; Wilson, M. A.; Fraser, J. S. Crystal Cryocooling Distorts Conformational Heterogeneity in a Model Michaelis Complex of DHFR. *Structure* **2014**, *22* (6), 899−910.
(29) Gray, H. B.; Winkler, J. R. Hole hopping through tyrosine/tryptophan chains protects proteins from oxidative damage. *Proc. Natl. Acad. Sci. U. S. A.* **2015**, *112* (35), 10920−10925.
(30) Winkler, J. R.; Gray, H. B. Electron flow through biological molecules: does hole hopping protect proteins from oxidative damage? *Q. Rev. Biophys.* **2015**, *48* (4), 411−420.
(31) Sun, W. C.; Dai, H. J.; Tao, Y.; Xiao, D.; Zhang, Y. F.; Wei, Z. D.; Chen, X. H. Potent Relay Stations for Electron Transfer in Proteins: pi therefore pi Three-Electron Bonds. *J. Phys. Chem. C* **2013**, *117* (36), 18325−18333.
(32) Edington, M. D.; Diffey, W. M.; Doria, W. J.; Riter, R. E.; Beck, W. F. Radiationless decay from the ligand-to-metal charge-transfer state in the blue copper protein plastocyanin. *Chem. Phys. Lett.* **1997**, *275* (1−2), 119−126.

DOI: 10.1021/acs.jpclett.7b02026
J. Phys. Chem. Lett. 2017, 8, 4498−4503